Design of simply structured metamaterial filters at sub-THz frequencies

Johanna Böhm[1,*], Karl Jacobs[1] and C.E. Honingh[1]
[1]*I. Physikalisches Institut, Universität zu Köln, 50937 Cologne, Germany*
[*]Contact: jboehm@ph1.uni-koeln.de

***Abstract*—We present simulation results of polarization sensitive filters for the sub-THz regime. The filters are designed following the principles of metamaterials.**

I. Introduction:

The increasing interest in Metamaterials (MM) combined with the development of highly efficient numerical simulation programs has caused an abundance of designs for various applications in recent years like perfect absorbers, negative refractive index material and invisible cloaks [1]–[4]. As the dimensions of single MM elements scale inversely with frequency the fabrication of designed MM devices are especially challenging for applications at higher frequencies. MMs are composed of sub-wavelength unit cells. Typically, they follows a periodically arrangement and consists of metallic resonators on dielectric layers. Considering the unit cells as "meta-atoms", their electromagnetic response is summed up in terms of homogenized parameters, e.g. the electric permittivity and magnetic permeability. This electromagnetic behavior strongly depends on the design of the sub-wavelength structures. Offering electromagnetic properties which are to a certain limit definable, MMs are especially interesting for applications at frequencies where the lack of suitable materials leads to challanging issues in the development of receiver and transmitter technologies [3]. Among others this includes the THz gap between 0.1 THz and 10 THz. The usage of MM based filters in this regime enables to significantly improve characteristics such as near 100 % in-band transmission which is important for the receiver applications, our filter designs are intended for. Our filter designs offer filter bands at about 300 GHz to 800 GHz. To enable a preferably straightforward fabrication process with reproducible results we use simple MM structures and restricts the number of available substrate layers to one, instead of multilayer stacked designs.

In the following section, we introduce the concept of our filter designs and present simulation results of one bandpass and one bandstop filter.

II. Design

Our filter designs are based on L-shaped resonators (LR). The excitation of the LR resonances strongly depends on the spatial alignment of the resonator arms to the **E**-field of the radiation source [5]. The two resonance modes, we concentrate on, can be easily distinguished by their oscillating surface currents as depicted in Fig.1. Mirror symmetric surface currents in both resonator arms indicate the symmetric mode. An incident **E**-field parallel to the axis of symmetry of the LR results in an exclusive excitation of this mode. Accordingly, the asymmetric mode is excited by an incident **E**-field aligned perpendicularly to the axis. An arbitrary aligned radiation causes a superposition of asymmetric and symmetric current flows in the resonator. Such an interplay of oscillations is able to yield polarization conversion [6]. The field amplitude **E** of the refracted radiation is cross-polarized (CR) if it is perpendicular to that of the incoming radiation. Co-polarized (CO) denotes the radiation with polarization direction parallel to the incident radiation.

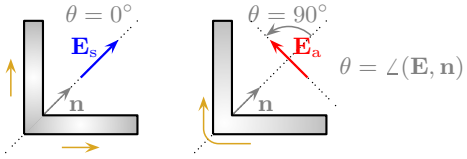

Figure 1. Sketch of two different resonance modes of the LR. The yellow arrows indicate the flows of current for the respective resonance (left: symmetric mode, right: asymmetric mode) The **E**-field vector indicates the relative orientation of an incoming radiation to the LR that is needed to only excite the specific mode. Θ is the alignment angle between the axis of symmetry of the LR and the **E**-field vector.

Table I
Dimensions of simulated filters

Filter	l_1 (µm)	p (µm)	h (µm)
Fig. 2(a)	82.7	100	9
Fig. 2(b)	79.3	92.8	14

$a = 5\,\mu m$ and $d = 2.5\,\mu m$ for all filter designs

III. Simulation Results

All calculations of the designed MM structures have been performed with the commercial simulation program CST Studio Suite [7] using the frequency domain solver of Microwave Studio. The results are given in terms of scattering parameters (S-parameters).

The filter design based on LRs provides at least two different filter bands. Changing the relative alignment of the filter with respect to the polarization of the incoming

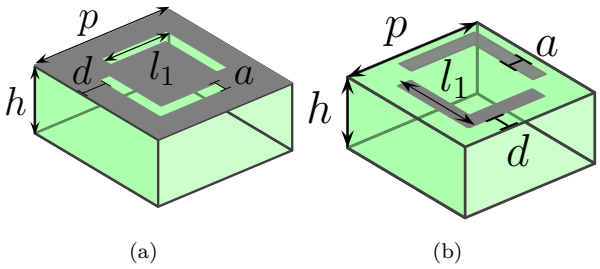

Figure 2. Dimensions of parameters for the bandpass filter design (a) and bandstop design(d). The dark-gray colored areas in the sketches indicate metal, the substrate is colored green.

radiation one can switch between the filter bands as depicted by the polarization alignment angle Θ in Fig. 1. We have designed one bandstop and one bandpass filter. To maximize the transmission behavior we use silicon membranes as substrate layers. They can be considered to be loss free within the sub-THz regime. The substrate is coated with LR structures on the front side (see Fig. 2). LRs placed on a loss free substrate, totally reflect an incident, linear polarized plane wave if only a single mode is excited. This provides the basis for the bandstop filter design. Following Babinet's principle [5], the reflective behavior can be transposed into a transmittive behavior when coating the substrate with the complementary image of the metal structures. Following this principle we realize the bandpass filter using LR slots instead of filled LRs. As a consequence the corresponding modes are excited when for the LR slots the **H**-field vector of the incoming radiation is positioned as the **E**-field vector for the LRs. A summary of the designs is given in Fig. 2 and Table I.

We have simulated the filtering performance using aluminum (conductivity 2.5×10^7 S/m) for all metal parts of the filters. For optimum alignment of the filter structures with the polarization of the incoming radiation, the simulation results predict a close to 100 % transmission of co-polarized radiation at the center frequency of the passbands as shown in Fig. 3 (a)-(b). The results for the bandstop filter given in Fig. 3 (c)-(d) show a suppression of the transmission of the co-polarized radiation of about −70 dB at the center frequency by reflecting all incoming radiation. The cross-polarized contributions of the radiation are not included in the graphics as they are less than −50 dB and can ne neglected in good approximation. Within an angle tolerance of ±10° there is no significant change in the filter performance.

A. Preliminary fabrication test

To study the stability of the filter and the design's suitability for fabrication we have first fabricated the filter structure of the bandpass filter on an available 15 µm thick substrate before processing on thinner wafers. The fabrication is performed on SOI wafers with a high resistivity silicon device layer (5 kΩ cm) on a 300 µm thick handle wafer. The filter structures are defined by standard photolithographic lift-off processes and deposition of 280 nm

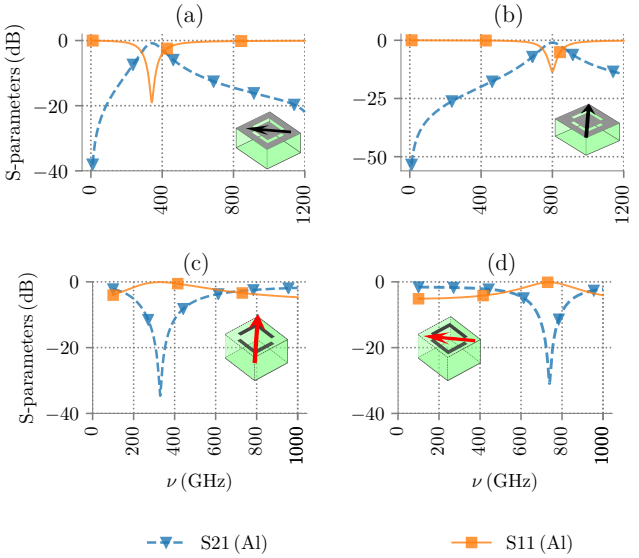

Figure 3. Simulation results of one bandpass (Fig. 2 (a)-(b)) and one bandstop filter design (Fig. 2 (c)-(d)). The left-hand column depicts the normalized amplitude magnitude of transmission S21 (dashed line with triangles) and reflection S11 (solid line with squares) of the lower filter bands and the column on the right those of the upper filter bands. The unit cells used for the filter designs are directly given in each diagram. An arrow shows the alignment of the filter geometries to the **E**-field vector (red) in case of the bandpass or the **H**-field vector (black) in case of the bandstop filter of the incoming linear polarized radiation.

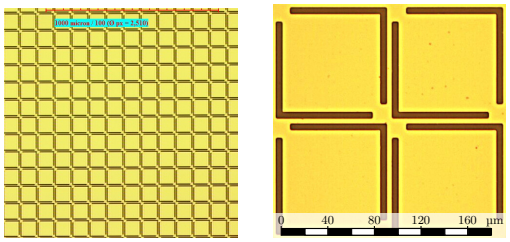

Figure 4. Photos of the bandpass filter for different zoom levels [9]. Dark brown colored: silicon layer. Bright yellow colored: aluminum.

aluminum on the front side. The handle wafer is etched away from the back side using Deep Reactive Ion etching in an SF_6 plasma, similar to what has been developed for our HEB mixers [8]. The final bandpass filter is circular with a diameter of 22.5 mm. It consists of more than 65 000 resonators (see Fig. 4) with only non-truncated LRs on its edges to prevent fringe effects.

IV. Conclusion

Based on simple L-shaped resonator geometries we have successfully designed a MM bandpass and bandstop filters for the sub-THz regime. Simulations of our designs predict very high transmission for the pass bands and low transparency for the stop filter.

Comparing commercially available filters for THz radiation [10] with the simulation predictions, the MM filters offer a higher performance with both an above-average

transmission and larger bandwidths. In comparison to MM filters that have been investigated for similar frequency ranges [11], [12] we find at least comparable, if not higher, filtering performance while using a significantly simpler design concept. An analysis of the alignment tolerances demonstrates a good practicability of the filters.The filters are currently being fabricated using SOI substrate technique and standard photolithography. Preliminary fabrication tests confirm processability even for huge numbers of L-resonators in the order of 10^4.

References

[1] H.-T. Chen, J. F. O'Hara, A. K. Azad, and A. J. Taylor, "Manipulation of terahertz radiation using metamaterials," *Laser & Photonics Reviews*, vol. 5, no. 4, pp. 513–533, 2011.

[2] N. I. Zheludev and Y. S. Kivshar, "From metamaterials to metadevices," *Nature materials*, vol. 11, no. 11, p. 917, 2012.

[3] H. Tao, W. J. Padilla, X. Zhang, and R. D. Averitt, "Recent progress in electromagnetic metamaterial devices for terahertz applications," *IEEE Journal of Selected Topics in Quantum Electronics*, vol. 17, no. 1, pp. 92–101, 2011.

[4] V. Veselago, L. Braginsky, V. Shklover, and C. Hafner, "Negative refractive index materials," *Journal of Computational and Theoretical Nanoscience*, vol. 3, no. 2, pp. 189–218, 04 2006.

[5] D. Lee and D.-S. Kim, "Light scattering of rectangular slot antennas: parallel magnetic vector vs perpendicular electric vector," *Scientific reports*, vol. 6, 2016.

[6] J. Ding, B. Arigong, H. Ren, J. Shao, M. Zhou, Y. Lin, and H. Zhang, "Mid-infrared tunable dual-frequency cross polarization converters using graphene-based l-shaped nanoslot array," *Plasmonics*, vol. 10, no. 2, pp. 351–356, 2014.

[7] CST - Computer Simulation Technology AG. CST - Computer Simulation Technology. [Online]. Available: https://www.cst.com/

[8] P. Pütz, K. Jacobs, M. Justen, F. Schomaker, M. Schultz, S. Wulff, and C. Honingh, "Nbtin hot electron bolometer waveguide mixers on Si3N4 membranes at thz frequencies," *IEEE Transactions on Applied Superconductivity*, vol. 21, no. 3, pp. 636–639, 2011.

[9] J. Böhm, "A metamaterial absorber for the sub-thz regime at cryogenic temperatures," *Master Thesis*, 2016.

[10] T. K. Ltd and Q. I. Ltd. Qmc instruments. [Online]. Available: http://www.terahertz.co.uk/qmc-instruments-ltd/thz-optical-components/multi-mesh-filters

[11] Q. Li, X. Zhang, W. Cao, A. Lakhtakia, J. F. O'Hara, J. Han, and W. Zhang, "An approach for mechanically tunable, dynamic terahertz bandstop filters," *Applied Physics A*, vol. 107, no. 2, pp. 285–291, 2012.

[12] M. Lu, W. Li, and E. R. Brown, "Second-order bandpass terahertz filter achieved by multilayer complementary metamaterial structures," *Optics letters*, vol. 36, no. 7, pp. 1071–1073, 2011.